Dielectric critical slowing down in pentakis(imidazolium) undecabromodibismuthate(III): $(C_3N_2H_5)_5Bi_2Br_{11}$

2009 J. Phys.: Condens. Matter 21 015904

(http://iopscience.iop.org/0953-8984/21/1/015904)

J. Phys.: Condens. Matter **21** (2009) 015904 (5pp) doi:10.1088/0953-8984/21/1/015904

Dielectric critical slowing down in pentakis(imidazolium) undecabromodibismuthate(III): $(C_3N_2H_5)_5Bi_2Br_{11}$

A Piecha and R Jakubas

Faculty of Chemistry, University of Wrocław, Joliot-Curie 14, 50-383 Wrocław, Poland

E-mail: rj@wchuwr.chem.uni.wroc.pl

Received 23 August 2008, in final form 29 October 2008
Published 1 December 2008
Online at stacks.iop.org/JPhysCM/21/015904

Abstract

Low frequency dielectric dispersion studies have been carried out for the ferroelectric pentakis(imidazolium) undecabromodibismuthate(III)—$(C_3N_2H_5)_5Bi_2Br_{11}$—single crystal in the paraelectric phase in the radio-frequency region (100 Hz–1 MHz). The dielectric dispersion, observed for an electric field along the a-axis ($P2_1/n$ space group), is characterized by a polydispersive nature close to the Curie temperature ($T_c = 155$ K). The dielectric dispersion findings were analyzed accurately with the Cole–Cole formula. In the vicinity of the Curie temperature the process of the dielectric critical slowing down is clearly observed. Such a dynamic dielectric response is characteristic of ferroelectric crystals classified as 'order–disorder' type.

1. Introduction

Organic–inorganic hybrid ferroelectrics are of growing interest for applications in opto-electronics as an useful materials for transistors, light-emitting devices, photovoltaic cells, and data storage [1–3]. Halogenoantimonates(III) and halogenobismuthates(III) of the general formula $R_aM_bX_{(3b+a)}$ (R, organic cations; M, trivalent metal ion—Sb or Bi; X, halogen), which are examples of such materials, have been extensively studied during recent years [4–7]. The crystal structure of these salts consists of a wide range of inorganic anions comprising an extended network of corner-sharing metal halide octahedral alternating with a variety of different organic cations. The anionic substructure is responsible for the thermal stability and mechanical flexibility of the materials whereas the organic moieties determine their electric properties.

Extensive experimental studies on the $R_aM_bX_{(3b+a)}$ (M = Sb (III), Bi(III)) family of crystals showed that ferroelectricity appears in the case of compounds characterized by two-dimensional anionic layers $(M_2X_9)^{3-}_{\alpha}$ [8–10]. On the other hand, several novel ferroelectric solid complexes were found to crystallize in the $R_5M_2X_{11}$ chemical composition, for which the anionic substructure consists of discrete bioctahedral units $[Bi_2X_{11}]^{5-}$. It is intriguing from the structural point of view that this type of anionic species is encountered quite rarely, and all compounds crystallizing with the $R_5M_2X_{11}$ composition reported to date appear to exhibit ferroelectric properties [11–14]. Since dielectric properties of the methylammonium analogs $(CH_3NH_3)_5Bi_2X_{11}$ (X = Cl, Br) are comparable to those found in well known TGS-type (triglycine sulfate) ferroelectrics, these materials still evoke much interest.

Recently, we reported on ferroelectric properties in three imidazolium compounds crystallizing with the chemical composition $(R)_5M_2X_{11}$, namely $(C_3N_2H_5)_5Bi_2Cl_{11}$ (abbreviation ICB) [15], $(C_3N_2H_5)_5Sb_2Br_{11}$ (IBA) [16] and $(C_3N_2H_5)_5Bi_2Br_{11}$ (IBB) [17]. All the crystals are isomorphous in the room temperature phase, crystallizing in the monoclinic space group, $P2_1/n$. Although they are isomorphous in the corresponding paraelectric phases (II), their sequence of phase transitions appeared to be different:

$$\text{ICB: } P\bar{4}n2 \xrightarrow{360\ \text{K}} P2_1/n\ (\text{I} \rightarrow \text{II}),$$

$$P2_1/n \xrightarrow{166\ \text{K}} P2_1\ (\text{II} \rightarrow \text{III})$$

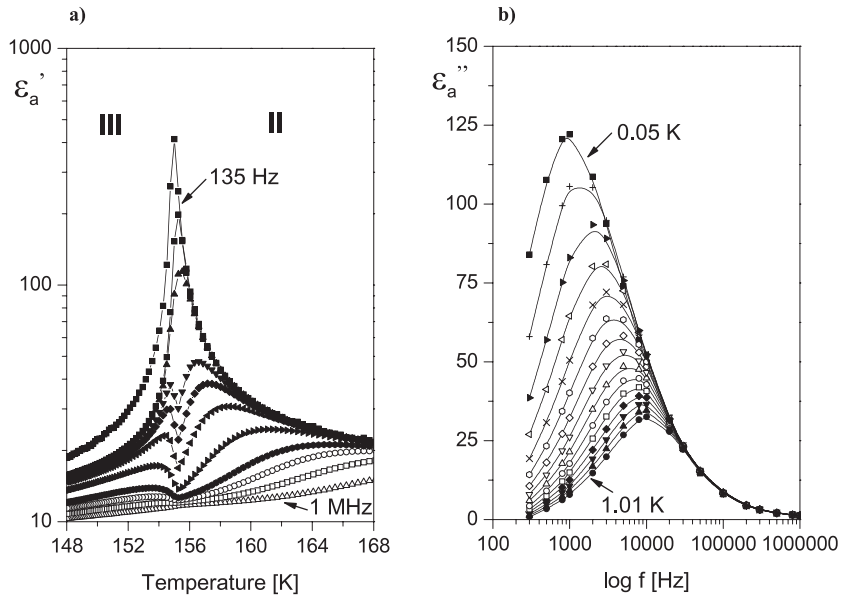

Figure 1. (a) Temperature dependence of the real part (ϵ_a') of the complex dielectric permittivity at selected frequencies along the a-axis near $T_c = 155$ K in the paraelectric phase (II). (b) Temperature dependence of the imaginary part of dielectric permittivity, ϵ_a'', at selected temperatures ($\Delta T = T - T_c$) in phase II of $(C_3N_2H_5)_5Bi_2Br_{11}$.

IBA: $P\bar{4}n2? \xrightarrow{360\ \mathrm{K}} P2_1/n$ (I $\rightarrow$ II),

$P2_1/n \xrightarrow{145\ \mathrm{K}} Pn$ (II $\rightarrow$ III),

$Pn \xrightarrow{120\ \mathrm{K}} Pn$ (III $\rightarrow$ IV)

IBB: $P\bar{4}n2? \xrightarrow{355\ \mathrm{K}} P2_1/n$ (I $\rightarrow$ II),

$P2_1/n \xrightarrow{155\ \mathrm{K}} Pn$ (II $\rightarrow$ III).

The lowest temperature phase (III) of IBB shows ferroelectric properties with the spontaneous polarization about 2.6×10^{-3} C m^{-2} (at 130 K) along the a-axis. It is postulated that the ferroelectric phase transition mechanism for all discussed crystals is due to the dynamics of the imidazolium cations [16, 17]. In this paper, we report the dynamic dielectric properties of the $(C_3N_2H_5)_5Bi_2Br_{11}$ single crystal in the paraelectric phase close to the Curie temperature ($T_c = 155$ K).

2. Experimental details

$(C_3N_2H_5)_5Bi_2Br_{11}$ was obtained from an aqueous solution of a stoichiometric mixture of imidazole amine and bismuth(III) tribromide with an excess of HBr acid. The single crystals of this compound were grown by a slow evaporation method at constant room temperature (25 °C).

The complex dielectric permittivity $\epsilon^* = \epsilon' - i\epsilon''$ was measured with an HP 4284A Precision LCR meter between 100 Hz and 1 MHz. The ac amplitude was 1 V. The samples for dielectric measurements were prepared by cutting the single crystal perpendicularly to the a-axis. The specimen with graphite electrodes had dimensions of $4 \times 4 \times 1$ mm^3. The error in the real and imaginary parts of the complex dielectric permittivities was less than 5%.

3. Results and evaluation

Figure 1(a) shows the temperature dependence of the real part of the complex dielectric permittivity, ϵ_a', at selected frequencies over the paraelectric phase, whereas figure 1(b) displays dielectric losses, ϵ_a'', versus frequencies at selected temperatures close to $T_c = 155$ K. From these figures it results that the dielectric dispersion becomes remarkable over the kilohertz frequency range (100 Hz–100 kHz). The experimental results in figures 1(a) and (b) were subsequently re-plotted as ϵ_a'' versus ϵ_a' (Cole–Cole plots) as presented in figure 2. This figure indicates that the dielectric relaxation is almost symmetric in nature. Therefore, the Cole–Cole relation:

$$\epsilon^* = \epsilon_\infty + \frac{\epsilon_0 - \epsilon_\infty}{1 + (i\omega\tau)^{1-\alpha}} \qquad (1)$$

was used to describe the dielectric response, where ϵ_0 and ϵ_∞ are the low and high frequency limits of the dielectric permittivity, respectively, ω is the angular frequency, τ is the characteristic relaxation time and α is a parameter which represents a measure of distribution of the relaxation times.

The fit parameters of the relaxation process for the crystal under investigation are given in table 1. The α parameter ranges from 0.04 up to 0.21 approaching T_c in the paraelectric phase. It indicates that a polydispersive nature of relaxation process (for $\alpha > 0.1$) is disclosed for temperatures $(T - T_c) < 0.5$ K. Mean relaxation time (τ—macroscopic) as a function of temperature in the close vicinity of the paraelectric–ferroelectric transition is shown in figure 3. The relaxation process in $(C_3N_2H_5)_5Bi_2Br_{11}$ is characterized by an apparent critical slowing down approaching T_c from above. A single soft mode relaxation time fulfills well the relation $\tau \propto (T - T_c)^{-1}$ (figure 3), over the temperature range about 3 K. It should be emphasized that such a behavior of the macroscopic relaxation

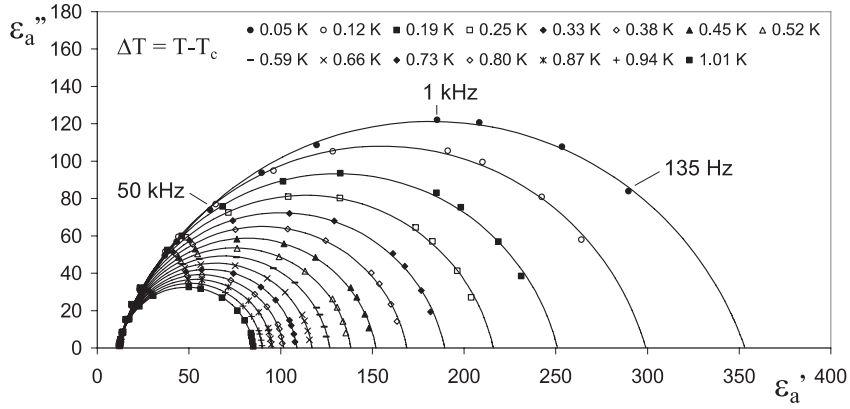

Figure 2. Cole–Cole plots of ϵ_a'' versus ϵ_a' at selected temperatures showing the relaxation nature of the dielectric dispersion in the paraelectric phase (II) of $(C_3N_2H_5)_5Bi_2Br_{11}$.

Table 1. Fit parameters of the relaxation process in $(C_3N_2H_5)_5Bi_2Br_{11}$. (The errors for the fitting parameters are the following: for τ and α about 10% and for ϵ_0 and ϵ_∞ about 5%.)

T (K)	ϵ_0	ϵ_∞	α	τ (10^5 s)
155.12	353.15	10.93	0.21	15.1
155.19	299.11	11.08	0.18	10.6
155.26	250.91	11.08	0.15	7.72
155.32	215.98	11.32	0.14	6.04
155.40	189.40	11.45	0.13	4.93
155.45	168.74	11.57	0.12	4.15
155.52	151.92	11.66	0.11	3.55
155.59	138.27	11.77	0.10	3.10
155.66	126.78	11.83	0.09	2.73
155.73	117.07	11.88	0.09	2.43
155.80	108.85	11.94	0.08	2.19
155.87	101.65	11.96	0.08	1.98
155.94	95.51	12.00	0.08	1.81
156.01	90.13	12.00	0.07	1.66
156.08	85.37	12.04	0.07	1.53
156.20	77.24	11.99	0.07	1.32
156.50	65.54	12.11	0.06	1.02
156.80	57.23	12.13	0.05	0.81
157.00	53.85	12.11	0.05	0.73
157.25	49.68	12.15	0.05	0.64
157.50	46.21	12.13	0.05	0.55
157.70	44.22	12.14	0.04	0.51

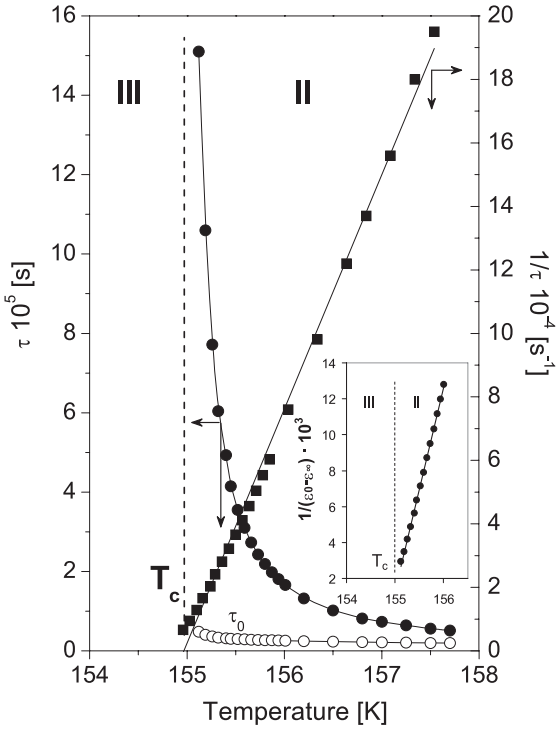

Figure 3. Temperature dependence of the macroscopic relaxation time (τ) and its inverse (τ^{-1}) above T_c (155 K) and τ_0 versus T. The inset shows the Curie–Weiss behavior of the static dielectric increment ($\Delta\epsilon = \epsilon_0 - \epsilon_\infty$).

time (τ) is typical of ferroelectric crystals classified as 'order–disorder' type.

The value of τ_0, characterizing the dielectric relaxator (single dipole), is related to the macroscopic relaxation time, τ, according to the formula [18]

$$\tau_0 = \frac{\tau\epsilon_\infty}{\epsilon_0 - \epsilon_\infty}. \quad (2)$$

It is found that the microscopic relaxation time (τ_0) for the analyzed relaxation process follows the Eyring relation:

$$\tau_0 = \frac{h}{kT}\exp\frac{\Delta E^*}{kT}. \quad (3)$$

In the temperature range $T > T_c + 0.5$ the activation free energy ΔE^* is estimated to be about 0.32 ± 0.05 eV (see figure 4). It should be noticed that the activation free energy ΔE^* increases significantly approaching T_c. Such a behavior is encountered in ferroelectric crystals in the paraelectric phase; nevertheless, this increase is rather large. The activation energy for $(C_3N_2H_5)_5Bi_2Br_{11}$ is comparable to those found from the relaxation studies for two other imidazolium analogs, $(C_3N_2H_5)_5Bi_2Cl_{11}$ and $(C_3N_2H_5)_5Sb_2Br_{11}$: 0.47 and 0.53 eV, respectively [15, 19]. Such large values of ΔE^* obtained for all imidazolium ferroelectrics may be explained in terms of possible specific interactions between this organic cation and anionic moieties and relatively large moments of inertia of reoriented bulky imidazolium cations. Our structural results showed that the imidazolium cations possessing two

Table 2. Comparison of the dielectric dispersion parameters in $R_5M_2X_{11}$-type ferroelectrics ($R = CH_3NH_3^+$—methylammonium, $C_6H_5NH^+$—pyridinium, $C_3N_2H_5^+$—imidazolium cations). (The τ, τ_0 and α parameters were estimated in the close vicinity of T_c.)

Cation	M(III)	X	T_c (K)	Frequency of dispersion	τ (s)	τ_0 (s)	α	ΔE^* (eV)
$CH_3NH_3^+$	Bi	Cl	307				0.01	0.11
$CH_3NH_3^+$	Bi	Br	312	10^6–10^9	$\sim 1 \times 10^{-8}$	$\sim 1 \times 10^{-10}$	0.02	0.12
$C_6H_5NH^+$	Bi	Br	118	2.5×10^1–10^4	1.3×10^{-3}	1×10^{-4}	0.11	0.29
$C_3N_2H_5^+$	Bi	Cl	166		1.3×10^{-4}	0.23×10^{-5}	0.21	0.47
$C_3N_2H_5^+$	Bi	Br	155	10^2–10^5	1.5×10^{-4}	0.48×10^{-5}	0.21	0.32
$C_3N_2H_5^+$	Sb	Br	145		4.6×10^{-4}	1.32×10^{-5}	0.23	0.39

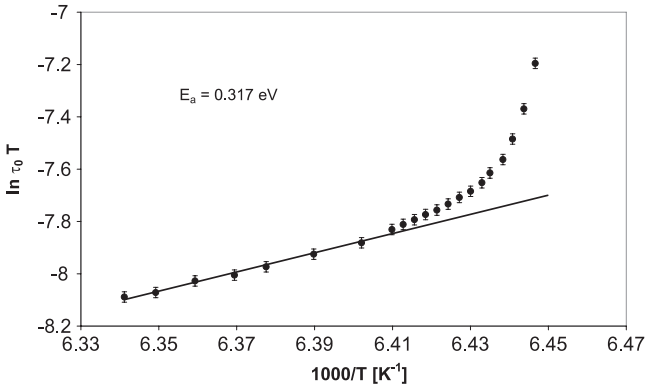

Figure 4. The activation energy obtained by means of the Eyring equation.

heteroatoms in the aromatic ring are used to form a complex network of hydrogen bonds. Thus the possible interactions can reduce the freedom of motions of cations in the lattice and result in a significant activation energy for the reorientation of dipoles.

4. Discussion

$R_5M_2X_{11}$-type ferroelectrics were found to form a typical molecular-ionic crystal. Their crystal structure consists of discrete bioctahedral units $(M_2X_{11})^{5-}$ and organic cations. The experimental studies showed that the cations seem to be exclusively responsible for the dynamic properties of these materials. The cationic substructure is quite complicated because there are present various structurally non-equivalent organic cations. Two of five cations (one type) placed in the general positions are ordered and are not expected to contribute to the critical dielectric properties in the paraelectric phase. On the other hand, the remaining three cations (three types) placed in the center of symmetry and being distributed over two positions in the paraelectric phase are postulated to contribute to the dynamic dielectric permittivity. These cations are indistinguishable at high temperatures because of high orientational disorder. Such a dynamic structural disorder is common for all ferroelectric crystals with $R_5M_2X_{11}$ composition. In the ferroelectric phases of these derivatives all cations were found to be ordered. The parameters characterizing the dynamic dielectric properties of this family of crystals are given in table 2.

Ferroelectric compounds belonging to the $R_5M_2X_{11}$ family (where R stands for organic cations such as: methylammonium, pyridinium and imidazolium) may be divided into two classes, which are characterized by different dynamic dielectric properties and phase transition sequences. The methylammonium analogs: $(CH_3NH_3)_5Bi_2Cl_{11}$ and $(CH_3NH_3)_5Bi_2Br_{11}$, crystallize in the paraelectric phase in the orthorhombic symmetry ($Pcab$). In the case of methylammonium derivatives, the relaxation process, taking place in the microwave frequency region, appears to be quite fast [20, 21]. It is interesting that the pyridinium and imidazolium derivatives were found to crystallize in their paraelectric phases in the monoclinic symmetry ($P2_1/n$). The relaxation process taking place in the audio-frequency region for these salts indicates an important slowing of motion of the aromatic cations near T_c in comparison to that found in the methylammonium salts. One can state that the differences in the geometry of the organic cations and the interactions between anionic and cationic substructures is reflected in the dynamic dielectric properties of these two various classes of crystals. The relatively large magnitude of ΔE^* and a long macroscopic relaxation time for the derivatives containing aromatic cations may be explained in terms of various possible hydrogen bond configurations and apparent steric effects. The imidazolium heteroatomic cations possess two protonodonor sites, thus they are able to form a three-dimensional network of the hydrogen bonds N–H $\cdots$ Br/Cl. The elongation of the relaxation times by nearly five to six orders, as compared with those found for the methylammonium analogs [20, 21], in our opinion is a result of fact that the organic moieties are much more strongly stabilized in the crystal lattice than the $CH_3NH_3^+$ ones. Static and dynamic dielectric properties of all imidazolium ferroelectrics ($R_5M_2X_{11}$ type), reveal significant similarities. The relaxation process taking place within the audio-frequency region is limited to the temperature region of about 2–3 K around T_c. The macroscopic relaxation time in all cases reveals a critical slowing down reaching about 10^{-3}–10^{-4} s close to T_c. The most striking feature of the imidazolium analogs is the fact that the characteristic ferroelectric relaxation process is extremely slow as compared to typical 'order–disorder' ferroelectrics [22], for which the relaxation process appears

usually in the microwave frequency region. There are known, however, some examples of order–disorder ferroelectrics characterized by a slow dynamics in their paraelectric phase, e.g. cyclohexane-1,1′-diacetic acid [23, 24] and $AgNa(NO_3)_2$ (τ close to T_c reaches about 4×10^{-4} s [25]). It should be emphasized that such an extremely slow motion limit is encountered rarely in ferroelectrics.

In conclusion, the dynamic dielectric properties of the crystal under investigation are common in all $R_5M_2X_{11}$ salts studied so far. The phenomenon of the critical slowing down which appears close to the Curie temperature in these ferroelectrics confirms clearly the order–disorder mechanism of the paraelectric–ferroelectric phase transitions.

Acknowledgment

This work was supported by the Polish State Committee for Scientific Research (Project Register No N204 108 31/2551).

References

[1] Lines M and Glass A M 1979 *Principles and Applications of Ferroelectric and Related Materials* (Oxford: Oxford University Press)
[2] Scott J F 2000 *Ferroelectric Memories* (Berlin: Springer)
[3] Russel V A, Evans C C, Li V and Ward M D 1997 *Science* **276** 575
[4] Jakubas R and Sobczyk L 1990 *Phase Transit.* **20** 163
[5] Jakubas R, Sobczyk L and Zaleski J 1997 *Polish J. Chem.* **71** 265
[6] Zaleski J and Pietraszko A 1996 *Acta Crystallogr.* B **52** 287
[7] Bujak M and Angiel R J 2005 *J. Solid State Chem.* **178** 2237
[8] Kallel A and Bats J W 1985 *Acta Crystallogr.* C **41** 1022
[9] Bujak M and Angel R J 2005 *J. Solid State Chem.* **178** 2237
[10] Jakubas R 1989 *Solid State Commun.* **69** 267
[11] Lefebvre J, Carpentier P and Jakubas R 1995 *Acta Crystallogr.* B **51** 167
[12] Matuszewski J, Jakubas R, Sobczyk L and Gowniak T 1990 *Acta Crystallogr.* C **46** 1385
[13] Jóźków J, Bator G, Jakubas R and Pietraszko A 2001 *J. Chem. Phys.* **114** 7239
[14] Jakubas R, Piecha A, Pietraszko A and Bator G 2005 *Phys. Rev.* B **72** 104107
[15] Piecha A, Bator G and Jakubas R 2005 *J. Phys.: Condens. Matter* **17** L411
[16] Piecha A, Pietraszko A, Bator G and Jakubas R 2008 *J. Solid State Chem.* **181** 1155
[17] Piecha A, Białońska A and Jakubas R 2008 *J. Phys.: Condens. Matter* **20** 325224
[18] Müser H E and Unruh H-G 1966 *Z. Naturf.* A **21** 785
[19] Piecha A and Jakubas R 2007 *J. Phys.: Condens. Matter* **19** 621
[20] Pawlaczyk C, Jakubas R, Planta K, Bruch C and Unruh H-G 1992 *J. Phys.: Condens. Matter* **4** 2695
[21] Pawlaczyk C, Planta K, Bruch C, Stephen J and Unruh H-G 1992 *J. Phys.: Condens. Matter* **4** 2687
[22] Blinc R and Zeks B 1974 *Soft Modes in Ferroelectrics and Antiferroelectrics* (Amsterdam: North-Holland) p 175
[23] Kroupa J, Vanek P, Krupkova R and Zikmund Z 1997 *Ferroelectrics* **202** 229
[24] Dolisek J, Arcon D, Kim H J, Seliger J, Zagar V, Vanek P, Kroupa J, Zikmund Z and Petzelt J 1998 *Phys. Rev.* B **57** R8063
[25] Grossmann J, Müller D, Petersson J and Schneider E 1976 *Z. Naturf.* a **31** 1089